Quantifying the probability of committed AMOC collapse

Philip B. Holden[1*], Jesse F. Abrams[2], Michelle Bieger[3], Timothy M. Lenton[2], Jean-Francois Mercure[2], Gregor Semieniuk[4], Simon Sharpe[5]

1. Environment, Earth and Ecosystems, The Open University, United Kingdom
2. Global Systems Institute, University of Exeter, United Kingdom
3. Transition Risk Exeter Ltd., United Kingdom
4. School of Public Policy and Department of Economics, University of Massachusetts Amherst, United States
5. S-Curve Economics, United Kingdom

* Corresponding author

E-mail: philip.holden@open.ac.uk

Abstract

The collapse of the Atlantic Meridional Overturning Circulation AMOC would have catastrophic consequences for societies. We quantify the risk of committed AMOC collapse using large ensembles of Earth system model simulations. Under conservative assumptions of Greenland ice sheet melt, the probability that collapse is already committed is 10%, rising to 80% by 2100 under worst case emissions. Under less conservative Greenland melt assumptions, probability that collapse is already committed is 23%.

Introduction

Projected AMOC responses under climate change are typically derived from ensembles of opportunity, usually climate model intercomparison projects (CMIP). Although recent studies have begun to focus upon and highlight the significant risk of collapse [1,2], studies have typically been projections of strength through time. From a risk-management perspective, a more appropriate approach is to assess the likelihood of crossing impact thresholds as a function of time [3], with particular focus on worst case scenarios [4]. This is partly motivated by the fact that it is challenging to make sufficiently accurate predictions for reliable decision-making. Ultimately it is the risk of worse case scenarios that matter, not projections of the exact state through time [5]. Here, we aim to improve upon this situation in two ways. Firstly, we focus on the outcome we want to avoid (AMOC collapse) and present our findings as the probability of that outcome through time. And secondly, we focus on the commitment to collapse rather than the ultimate collapse itself. These two changes make the timing, scale and likelihood both easier to understand and more relevant to decision-making.

To define committed collapse, i.e. that past and unavoidable future emissions have already locked in collapse, we assume that global emissions cannot be mitigated from peak to net-zero any faster than 35 years. This choice was motivated by techno-economic-climate modelling which demonstrated that a transition to net zero faster than 30 years was precluded under plausible policy and technological assumptions, even with the inclusion of optimistic negative emission assumptions [6,7]. In the 50 C1 no-overshoot 1.5°C scenarios of IPCC AR6 that report this data [8], only 12% are faster than 35 years, and none faster than 30 years.

To quantify committed collapse, we perform a series of ensembles of simulations. We assume that emissions beyond 2005 follow RCP8.5 until the year of peak emissions and are then mitigated linearly to zero over 35 years. Although the long-term realism of RCP8.5 has been questioned, it provides a good fit to cumulative emissions to 2020, and it provides a worst-case future scenario appropriate for risk assessment. All simulations are run for 300 years, spun on from historical transients (1805 to 2005). Each ensemble corresponds to some year of peak emissions, which we vary from 2005 to 2135 at intervals of ten years. The '2025 peak ensemble' therefore quantifies the probability that AMOC collapse is already committed, i.e. past emission have already locked in the collapse by 2025; this is simply calculated as percentage of simulations which collapse under the assumption that emissions will reduce linearly to net-zero in 2060. The choice to use RCP8.5 as the baseline profile ensures that our ensembles span the cumulative emissions of the RCPs. To illustrate, the 2025 peak ensemble has 456 GtC emissions (2005-2100 CE), which compares to 382GtC in RCP2.6. Peak warming is controlled by cumulative emissions [9], although our assumptions bring forward its timing, as our emissions profiles are generally front-loaded relative to the

RCP with most similar emissions. We include counter-factual experiments with emissions peaking in 2005 and 2015, in part to fully span the RCPs; the 2015 peak ensemble has cumulative emissions of 292 GtC.

To quantify uncertainties associated with these baseline projections, we perform sensitivity ensembles to explore i) the role of increased Greenland meltwater rate [10], noting our baseline assumes the melt rate derived from ISIMIP under RCP8.5 [11], and ii) slower future emissions trajectories, testing the conservative idealised assumption of historical emissions to 2024 [12] and flat thereafter until mitigation over 35 years commences in 2035, 2045 and 2055.

The experiment is computationally demanding, requiring twenty-one 69-member ensembles of 300-year simulations, representing more than 400,000 model years, thereby necessitating a computationally efficient Earth system model. We use PLASIM-GENIE [13], a low-resolution (~5°), intermediate-complexity, fully-3D coupled atmosphere-ocean model. This minimum level of complexity is needed to represent coupled ocean and atmosphere dynamics, noting that AMOC stability depends upon the net transport of moisture from the Atlantic to the Pacific, which contributes to the elevated surface salinity of the Atlantic. Models with simplified atmospheric dynamics fail to capture this moisture flux of ~0.4 Sv [14], requiring flux correction. They also lack feedbacks that are fundamental to AMOC stability. In contrast, all PLASIM-GENIE ensemble members simulate realistic AMOC without flux correction [7].

To perform the probabilistic analysis, we apply a perturbed parameter ensemble [7] which was carefully designed through a ‘history matching’ calibration [15], an approach

which samples throughout high-dimensional model input space to identify model configurations that produce plausible simulations, only ruling out simulations that are clearly inconsistent with data after allowing for model error. This approach avoids the introduction of bias through over-fitting and generates an ensemble that encompasses the full range of realistic dynamical feedbacks implemented in the model. The history-matched ensemble has been shown to display uncertainties in transient climate sensitivity, carbon-cycle sensitivity and AMOC stability which capture well the spread of high-complexity models [7]. Under RCP8.5 with no Greenland melt forcing, the simulated AMOC weakens by 16% to 54% over the period 1990-2090 (90% confidence) [7], which compares to a range of 15% to 60% in CMIP5.

Methods

The Earth system model

PLASIM-GENIE is a coupling of the intermediate-complexity spectral atmosphere model PLASIM [16] to the frictional geostrophic ocean model GOLDSTEIN [17] through the Grid-Enabled Integrated Earth system model GENIE [18]. The coupling and climatology are described in detail in [13]. PLASIM-GENIE is not flux corrected [7]. We apply the model with carbon-coupled biosphere modules BIOGEM and ENTS, described in [18]. We apply BIOGEM with the default Michaelis-Menton phosphate-limited productivity scheme [19]. The carbon-cycle model has been extensively validated through model inter-comparisons [20,21], while the climate-carbon cycle of our specific PLASIM-GENIE configuration was validated in [7].

We performed PLASIM-GENIE ensembles using the 69-member 'history-matched' parameter sets, varying 31 key model parameters across their plausible input ranges [22], and selected from hundreds of millions of randomly sampled parameter configurations using emulation [7]. These parameter sets all simulate ten key global-scale observational targets of surface air temperature, vegetation and soil carbon, Atlantic, Pacific and Southern Ocean circulation metrics, dissolved ocean oxygen concentration, deep ocean calcium carbonate flux, and historically forced transient temperature and atmospheric CO_2 changes relative to preindustrial.

The AMOC diagnostic applied was maximum of the Atlantic overturning stream function below 500m. The mean preindustrial strength across the ensemble is 20.8±1.9 Sv. We define that collapse has occurred when this diagnostic falls below 45% of preindustrial strength. This value represents a proxy for the unstable AMOC regime in this model, noting that only 26 of the 868 simulations in the baseline ensembles have minimum AMOC strengths between 40% and 50% of preindustrial strength. The preindustrial and collapsed stream functions of the six simulations committed to collapse in the 2025 ensemble are plotted in Supplementary Figure 1, showing in each case the strong preindustrial overturning cell is weakened and shifted to lower latitudes, with the 6 Sv contour lying south of 40°N, indicating a major reduction in heat transport to higher northern latitudes.

Supplementary Figure 1. Preindustrial and collapsed Atlantic Meridional streamfunctions for the six simulations committed to AMOC collapse in 2025. Each row shows a single model set (ID labelled in the collapsed panel), with the preindustrial streamfunction (left) and the collapsed streamfunction at the year of collapse (right; year

labelled). Colour scale shows overturning strength in Sverdrups (Sv). In all six cases, the strong preindustrial overturning cell which is centred in the mid-to-high North Atlantic is absent in the collapsed state, replaced by a weakened, southward-shifted residual circulation with the 6 Sv contour lying south of 40°N. The vertical blue line marks 40°N for reference. Collapse years range from 2065 to 2205, illustrating the multi-decadal to centennial delay between commitment (by 2025) and the physical collapse event.

Experimental design

Each model configuration was spun-up with a 2,000-year atmosphere-ocean-geared quasi-equilibrium preindustrial simulation, with atmospheric CO_2 relaxed to 278ppm. Simulations were continued as emissions-forced historical transient simulations (atmosphere-ocean gearing off, CO_2 freely evolving). Historical forcing (1805 to 2005) comprised anthropogenic CO_2 emissions and non-CO_2 radiative forcing. Fossil fuel, cement and gas flaring emissions were from CMIP5 (https://cmip.llnl.gov/cmip5/forcing.html) and were combined with ISAM C-N land-use change emissions [23] from the HYDE land-use dataset [24]. Non-CO_2 forcing data was taken from [25] implemented in PLASIM-GENIE as effective CO_2.

For the baseline ensembles, post-2005 CO_2 emissions, land use change emissions and non-CO_2 radiative forcing were taken from the RCP8.5 scenario and linearly extrapolated from 2105 out to 2135. The Greenland meltwater flux follows a linear ramp which integrates to 90mm sea level rise contribution at 2100, the central estimate of ISIMIP6 under RCP8.5 forcing [11]. We perform fourteen 69-member ensembles following this forcing, with emissions peaking at decadal intervals from 2005 through to 2135. From the time of peak

emissions, CO_2 emissions and radiative forcing are reduced linearly to zero over 35 years and meltwater is held constant for the remainder of the simulation.

To test sensitivity to faster Greenland melt rate assumptions, the ensemble with 2025 peak emissions was repeated with a fixed freshwater flux that gives 274 mm sea level rise by 2100, the committed melt rate estimate of [10]. For the 2105 peak emissions ensemble (following RCP8.5), a high-end melt rate was derived by following the linear ramp of the baseline profile but scaled to the flux derived above from [10] in 2025 and giving a 427 mm sea level rise contribution by 2100.

To test more conservative emissions profiles, we performed ensembles with historical emissions to 2024 [12] and held constant thereafter (at 11.79 GtC yr^{-1}) until the assumed start of mitigation to zero over 35 years in 2035, 2035 and 2045. For these three ensembles, the Greenland melt rate was assumed to follow the baseline profile until year of mitigation start, after which it was held fixed, equating to 62 mm, 70 mm and 77 mm sea level rise respectively by 2100.

In summary, we performed 23 experiments, comprising 14 baseline experiments following RCP8.5 with ISIMIP Greenland melt fluxes, four Greenland meltwater sensitivities and three emissions sensitivities, being historical emissions to 2024, held fixed going forward until start of mitigation. Sixty-two parameter sets successfully completed all 23 experiments and analysis considers only the simulations from those 62 parameter sets.

Results

Figure 1 summarises the 14 baseline ensembles, with emissions peaking from 2005 through to 2135. Figure 1a plots the forcing, illustrated for the specific example of 2105 peak emissions under RCP8.5, with CO_2 emissions and non-CO_2 radiative forcing linearly reduced to zero over 35 years at 2140 and with Greenland meltwater flux held constant after peak emissions. Figure 1b plots the peak warming from the 62 simulations in each ensemble, noting that seven of the 69 parameter sets were not included because they did not successfully complete in all 14 ensembles. The assumption of 2025 peak-emissions just fails to meet the most ambitious no-overshoot 1.5°C target of the Paris Agreement, with 43% of the simulations remaining below 1.5°C decadal-averaged peak warming relative to preindustrial. Figure 1c plots the minimum AMOC strength relative to preindustrial as a function of peak warming and demonstrates the bistable nature of the AMOC, being in either a functioning "on" state or a fully collapsed "off" state, with very few simulations remaining in the intermediate regime around 45% of preindustrial strength. Warming both weakens the "on" state and increases the likelihood of the "off" state. The probability of collapse as a function of peak warming (Figure 1d) highlights the benefits of meeting the Paris targets; the probability of collapse rises steeply above 2°C of peak warming.

Figure 1. Forcing, ensemble spread, and bi-stability across peak-emission ensembles. (a) Illustrative forcing scenario for the 2105 peak-emissions ensemble. CO_2 emissions and non-CO_2 radiative forcing follow RCP8.5 to 2105, then decline linearly to zero over 35 years (by 2140). Greenland meltwater flux is fixed from 2105 and held constant for the remainder of the 300-year simulation. Units are given in the legend. (b) Peak warming (relative to preindustrial) across all 62 parameter sets for each of the 14 baseline ensembles, plotted against the year of peak emissions. (c) Minimum AMOC strength (relative to preindustrial) as a function of peak warming, showing the bistable character of AMOC: simulations cluster in

either an "on" state (>45% of preindustrial strength) or a collapsed "off" state, with few trajectories remaining in the unstable intermediate regime. (d) Probability of AMOC collapse as a function of peak warming, illustrating the strong non-linearity and the disproportionate risk-reduction benefits of meeting the Paris targets.

In Figure 2, we move from expressing the risk metrics in terms of peak warming to expressing them in terms of the year of peak emissions, which is more useful from a policy perspective. The probability of committed AMOC collapse is already 10% (at 2025) and rises to 82% by the end of the century under RCP8.5 (Figure 2a). The preindustrial and collapsed stream functions of the six simulations already committed to collapse (Supplementary Figure 1) show in each case the strong preindustrial overturning cell weakened and shifted to lower latitudes, with the 6 Sv contour lying south of 40°N. These six simulations have a mean modern AMOC strength of 87±4% of preindustrial, compared to 92±5% across the full ensemble, and an observation-based estimate of 85±5% [26]; ensemble members with strengths that are most consistent with observations are disproportionately represented among those already committed to collapse, suggesting that a 10% probability of committed AMOC collapse may be conservative. Under higher committed Greenland ice sheet melt rates [10], the probability of already-committed collapse rises to 23% at 2025, increasing to 100% by the end of century. Under (implausible) no-meltwater scenario probabilities are 3% in 2025 increasing to 61% by the end of the century; these are included partly to demonstrate that Greenland meltwater is not necessary to initiate collapse in this model. The risk of collapse continues to increase under flattened emissions (light blue data points in Fig. 2a) which are derived from an assumption of historical emissions to 2024 and fixed thereafter until they decline over 35 years from 2035, 2045, or 2055.

Figure 2. Probability and timing of committed and actual AMOC collapse through time. (a) Probability that AMOC collapse is already committed, as a function of the assumed year of peak emissions. The main curve (solid black) uses the baseline ISIMIP Greenland meltwater flux; vertical dashed lines at 2025 and 2105 indicate the spread between a high-melt scenario [10] (upper bound) and a no-meltwater counterfactual (lower bound). Light blue data points (2035–2055) show probabilities under the flat-emissions sensitivity, in which historical emissions are held constant until mitigation commences. Under the baseline, the probability of committed collapse rises from 10% in 2025 to 82% by 2100. (b) Year of actual AMOC collapse (first year at which AMOC strength falls to 45% below preindustrial) as a function of the committed year (the earliest year of peak emissions that drives that collapse), for the simulations that collapse. The mean delay between commitment and actual collapse is 84±38 years, with the earliest collapse occurring around 2060. (c) AMOC strength time series for all 62 simulations in the 2025 peak-emissions ensemble. (d) As (c), for the 2105 peak-emissions ensemble.

Figure 2b illustrates the year of actual collapse, defined as the year when the simulated AMOC strength is first 45% lower than the preindustrial average, as a function of the committed year – the earliest year of peak emissions under which this collapse is unavoidable. The average delay from committed year to the year of actual collapse is 84±38 years. The earliest collapse occurs at around 2060. Thus, the commitment to AMOC collapse could already be irreversible while the consequences remain decades away. Importantly, even after collapse is committed, mitigation remains urgent; if emissions continue unabated for an additional ten years beyond the point of commitment, the delay until actual collapse is reduced sharply (from 84±38 years) to 57±21 years. Figures 2c and 2d illustrate the time series for the 2025 and 2105 peak emission ensembles with the baseline Greenland melt.

Discussion and Conclusions

The IPCC sixth assessment report characterised AMOC change primarily through projections of weakening strength, concluding that AMOC is likely to decline by 24–39% by 2100 under moderate-to-high emissions (central estimates), a figure recently revised upward to ~50% [2]. However, this may obscure the risk that AMOC poses, which is an irreversible state transition on human timescales, with abrupt consequences for European temperatures, tropical monsoon systems, and sea level along the eastern North American seaboard, with changes happening at rates that would be highly challenging for adaptation. Our analysis shows that there is a >10% probability that collapse is already committed, regardless of the speed of any feasible future mitigation, and rising steeply under continued emissions.

References

1. Drijfhout S. *et al* Shutdown of northern Atlantic overturning after 2100 following deep mixing collapse in CMIP6 projections *Environ. Res. Lett.* **20** 094062 (2025) 10.1088/1748-9326/adfa3b

2. Portmann V., Swingedouw, D., Khattab, O. and Chavent M. Observational constraints project a ~50% AMOC weakening by the end of this century. *Sci. Adv.***12**, eadx4298 (2026). 10.1126/sciadv.adx4298

3. Sharpe, S. Telling the boiling frog what he needs to know: why climate change risks should be plotted as probability over time, *Geoscience Communication*, **2**, 95–100, (2019) https://doi.org/10.5194/gc-2-95-2019

4. Stott, P.A. *et al.* We need a global assessment of avoidable climate-change risks *Nature* **650**, 826-828 (2026) *https://doi.org/10.1038/d41586-026-00544-6*

5. Mercure, J.-F, et al. Risk-opportunity analysis for transformative policy design and appraisal, Global Environmental Change, **70**, 102359 (2021) https://doi.org/10.1016/j.gloenvcha.2021.102359

6. Mercure, J.-F. et al. Macroeconomic impact of stranded fossil fuel assets, *Nature Climate Change*, **8**, 588–593 (2108) https://doi.org/10.1038/s41558-018-0182-1

7. Holden, P. B. et al. Climate-carbon cycles uncertainties and the Paris Agreement. *Nat. Clim. Change* **8**, 609–613 (2018) https://doi.org/10.1038/s41558-018-0197-7

8. Byers, E., et al. 2022. *AR6 Scenarios Database hosted by IIASA*. International Institute for Applied Systems Analysis, 2022. doi: 10.5281/zenodo.5886911

9. Allen, M. *et al.* Warming caused by cumulative carbon emissions towards the trillionth tonne. *Nature* **458**, 1163–1166 (2009)
https://doi.org/10.1038/nature08019

10. Box J.E. *et al.* Greenland ice sheet climate disequilibrium and committed sea-level rise Nature Climate Change **12** 808-813 (2022)
https://doi.org/10.1038/s41558-022-01441-2

11. Goelzer H. *et al.* The future sea-level contribution of the Greenland ice sheet: a multi-model ensemble study of ISMIP6 The Cryosphere 14 3071-3096 (2020)
https://doi.org/10.5194/tc-14-3071-2020

12. Friedlingstein P. et al., Global Carbon Budget 2025, *Earth System Science Data*, in review, 2025
https://doi.org/10.5194/essd-2025-659

13. Holden, P.B. *et al.* PLASIM–GENIE v1.0: a new intermediate complexity AOGCM *Geosci. Mod. Dev.* **9** 3347-3361 (2016)
https://doi.org/10.5194/gmd-9-3347-2016

14. Craig P.M., Ferreira, D. and Methven, J. The contrast between Atlantic and Pacific surface water fluxes Tellus **69** 1330454 (2017)
https://doi.org/10.1080/16000870.2017.1330454

15. Williamson, D. et al. History matching for exploring and reducing climate model parameter space using observations and a large perturbed physics ensemble. *Clim. Dyn.* **41**, 1703–1729 (2013).

16. Fraedrich, K. A suite of user-friendly climate models: Hysteresis experiments *Eur. Phys. J. Plus* **127**, 53 (2012)

17. Edwards NR and Marsh R Uncertainties due to transport-parameter sensitivity in an efficient 3-D ocean-climate model. *Clim Dyn* **24**, 415–433 (2005) doi:10.1007/s00382-004-0508-8

18. Lenton, T. M. *et al.* Millennial timescale carbon cycle and climate change in an efficient Earth system model *Climate Dynamics* **26**, 687–711 (2006)

19. Ridgwell, A. *et al.* Marine geochemical data assimilation in an efficient Earth System Model of global biogeochemical cycling *Biogeosciences* **4**, 87–104 (2007)

20. Joos, F. *et al.* Carbon dioxide and climate impulse response functions for the computation of greenhouse gas metrics: a multi-model analysis *Atmos. Chem. Phys.* **13**, 2793-2825 (2013)

21. Zickfeld, K. et al. Long-term climate change commitment and reversibility: An EMIC intercomparison *J. Climate* **26**, 5782– 5809 (2013)

22. Holden, P.B. et al. PALEO-PGEM v1.0: a statistical emulator of Pliocene–Pleistocene climate, *Geosci. Model Dev.*, 12, 5137–5155 (2019)

23. Jain, A. K., Meiyappan, P., Song, Y., and House, J. I. CO_2 Emissions from land-use change affected more by nitrogen cycle, than by the choice of land cover Data *Global Change Biology* **19**, 2893-2906 (2013)

24. Ramankutty, N., Evan, A. T., Monfreda, C., and Foley, J. A. (2008), Farming the planet: 1. Geographic distribution of global agricultural lands in the year 2000, *Global Biogeochem. Cycles*, 22, GB1003 (2008)

25. Meinshausen, M. *et al.* The RCP greenhouse gas concentrations and their extensions from 1765 to 2300. *Climatic Change* **109**, 213-241 (2011)

26. Caesar, L. *et al.* Observed fingerprint of a weakening Atlantic Ocean overturning circulation. *Nature* **556**, 191–196 (2018)
https://doi.org/10.1038/s41586-018-0006-5

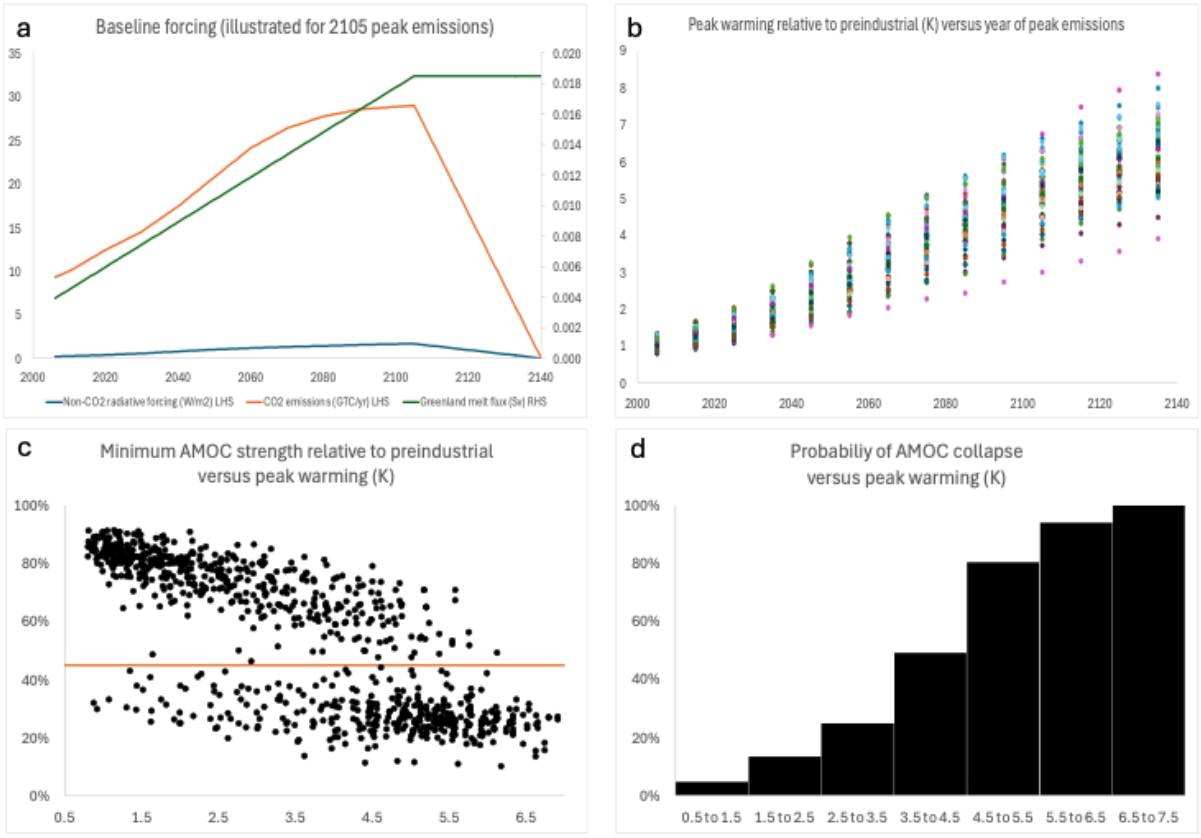

Figure 1. Forcing, ensemble spread, and bi-stability across peak-emission ensembles.

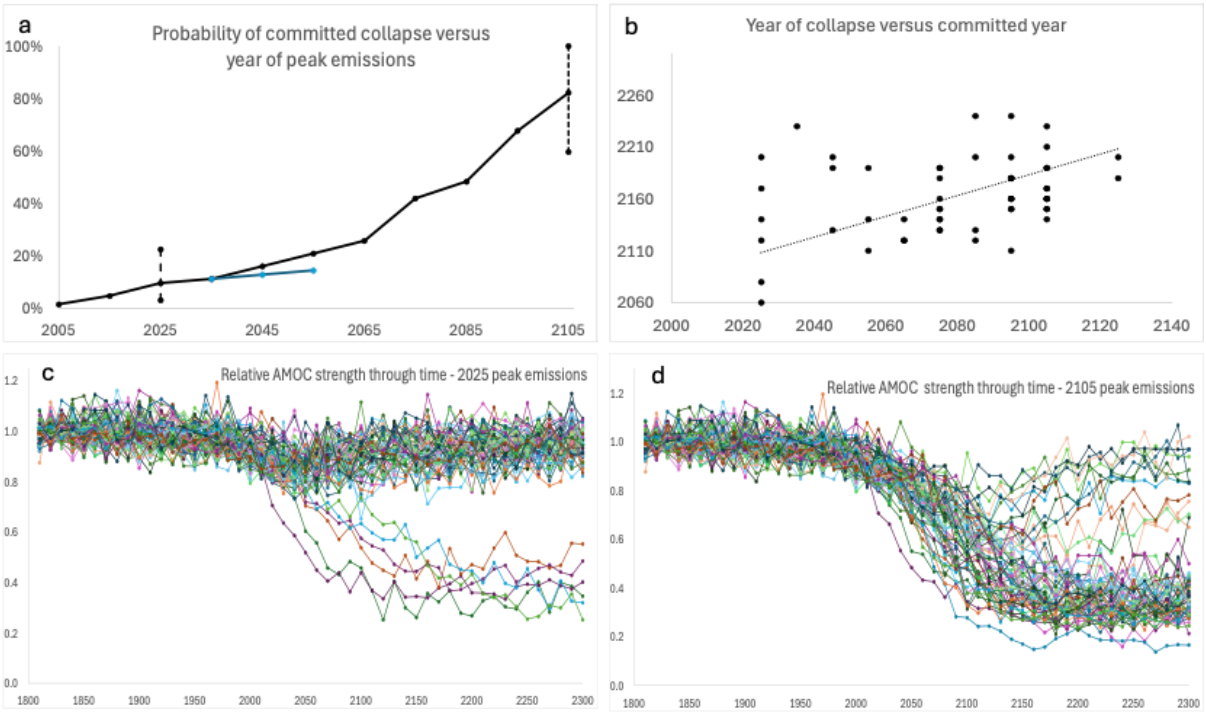

Figure 2. Probability and timing of committed and actual AMOC collapse through time.

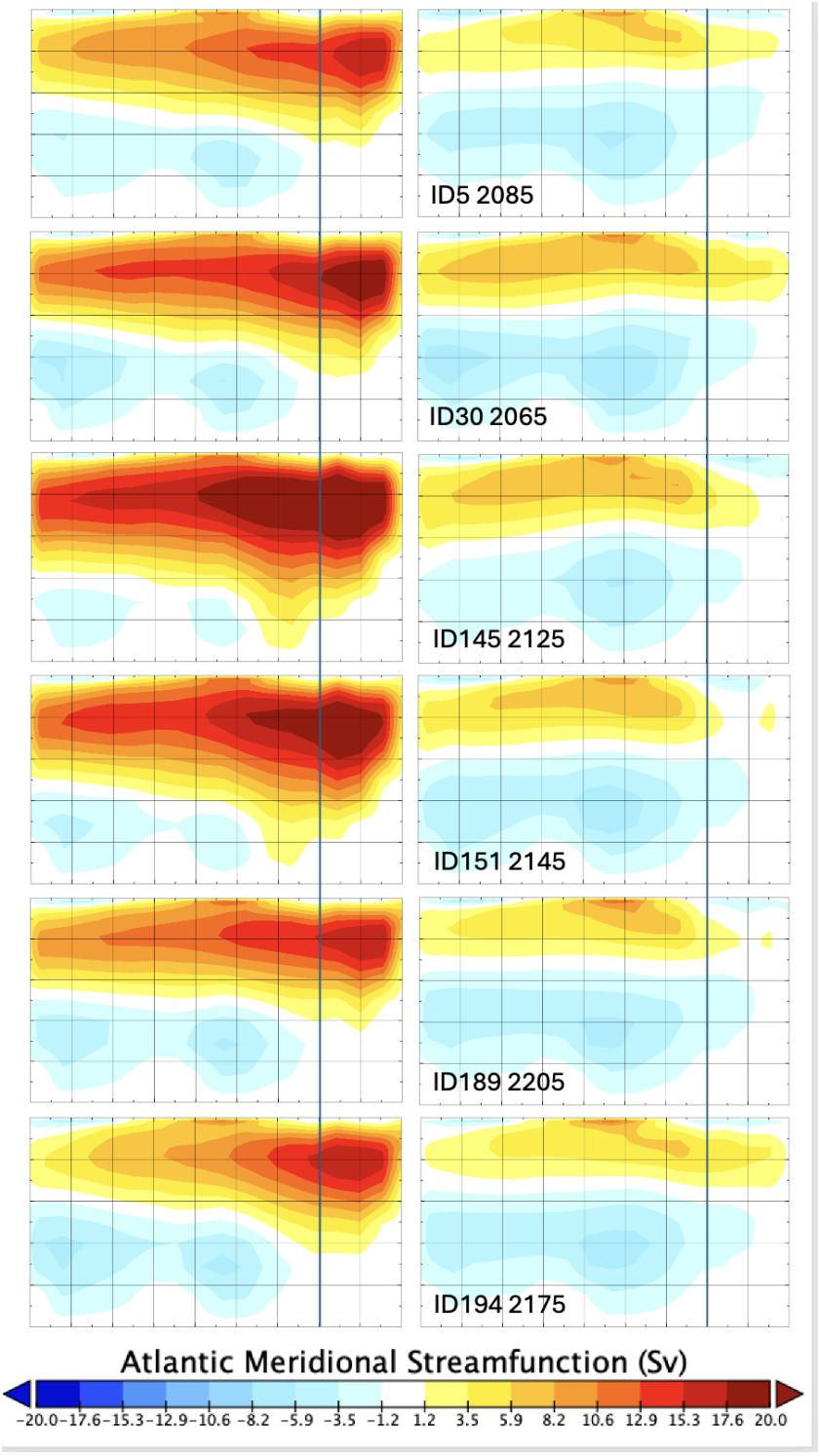

Supplementary Figure 1. Preindustrial and collapsed Atlantic Meridional streamfunctions for the six simulations committed to AMOC collapse in 2025.